



Proceeding Paper

# Electronic Structures and Photovoltaic Properties of Copper-, Sodium- and Ethylammonium-Added $\text{CH}_3\text{NH}_3\text{PbI}_3$ Perovskite Compound <sup>†</sup>

Riku Okumura <sup>1</sup>, Takeo Oku <sup>1,\*</sup> , Atsushi Suzuki <sup>1</sup> , Masanobu Okita <sup>2</sup>, Sakiko Fukunishi <sup>2</sup>, Tomoharu Tachikawa <sup>2</sup> and Tomoya Hasegawa <sup>2</sup>

<sup>1</sup> Department of Materials Science, The University of Shiga Prefecture, 2500 Hassaka, Hikone 522-8533, Shiga, Japan

<sup>2</sup> Osaka Gas Chemicals Co., Ltd., 5-11-61 Torishima, Konohana-ku, Osaka 554-0051, Osaka, Japan

\* Correspondence: oku@mat.usp.ac.jp; Tel.: +81-749-28-8368

† Presented at the 3rd International Electronic Conference on Applied Sciences, 1–15 December 2022;

Available online: <https://asec2022.sciforum.net/>.

**Abstract:** Copper, alkali metals, and organic cations were added to perovskite precursor solutions to enhance the photovoltaic conversion properties and durability of perovskite solar cells. Device properties were improved by the co-addition of copper and sodium. The enhancement of open-circuit voltage by bromine substitution also contributed to the improvement of conversion efficiency. First-principles calculations indicated that the energy levels derived from the Cu d orbital would function as an acceptor level. While the conversion efficiency of the device increased, the durability of the device decreased. Considering the results of the first-principles calculation, the decrease in device durability was attributed to the instability of the crystal structure due to the Cu and sodium substitutions. To enhance the crystal stability, ethylammonium was introduced as a stable organic cation, and the addition of ethylammonium to the perovskite precursor solution significantly enhanced the device's durability while maintaining conversion efficiency.

**Keywords:** copper; sodium; ethylammonium; first-principles calculations; perovskite; solar cell



**Citation:** Okumura, R.; Oku, T.; Suzuki, A.; Okita, M.; Fukunishi, S.; Tachikawa, T.; Hasegawa, T. Electronic Structures and Photovoltaic Properties of Copper-, Sodium- and Ethylammonium-Added  $\text{CH}_3\text{NH}_3\text{PbI}_3$  Perovskite Compound. *Eng. Proc.* **2023**, *31*, 29. <https://doi.org/10.3390/ASEC2022-13778>

Academic Editor: Maria Pesavento

Published: 1 December 2022

**Publisher's Note:** MDPI stays neutral with regard to jurisdictional claims in published maps and institutional affiliations.



**Copyright:** © 2022 by the authors. Licensee MDPI, Basel, Switzerland. This article is an open access article distributed under the terms and conditions of the Creative Commons Attribution (CC BY) license (<https://creativecommons.org/licenses/by/4.0/>).

## 1. Introduction

Much research has been conducted to improve the conversion efficiency and durability of perovskite solar cells. In addition to experimental investigations of the effects of compound addition, first-principles calculations are also being actively used to predict the properties of perovskite solar cells. In this study, experiments and first-principles calculations were performed in parallel, and the results of the calculations were used to investigate the effects of compound additions obtained from experiments.

Here, the effects of adding copper (Cu), alkali metals, and organic cations are investigated. It has been reported that the addition of Cu compounds to perovskite precursor solutions improves the film quality of perovskite films by increasing the grain size and homogenizing the surface morphology [1–3]. In addition, each cationic species of alkali metal has its own specific additive effect [4–6]. For example, the reduction of hysteresis by the introduction of potassium cation [7] and the homogenization of halogen distribution by the introduction of rubidium cation [8] have been reported.

Co-addition of Cu and alkali metals to perovskite precursor solutions has been reported to improve device conversion efficiency and durability [9,10]. However, first-principles calculations revealed that the substitution of Cu and Na destabilizes the crystal structure. Therefore, we suggested the introduction of stable organic cations to improve the stability of the crystal structure [11]. In a previous study, it was shown that the crystal structure of  $\text{CH}_3\text{NH}_3\text{PbI}_3$ , a standard perovskite crystal known as a photoelectric conversion

material, can be stabilized by substituting methylammonium (MA) with ethylammonium (EA) [12]. In experiments, it was also reported that the introduction of EA compounds enhanced the durability of the devices [13,14].

The composition of halogens in perovskite crystals is also very important, and halogens are known to affect mainly the energy gap. There are a number of studies that have investigated the effect of halogen composition [15–17].

The purpose of this study is to investigate the effects of adding Cu, Na, and EA to perovskite precursor solutions using first-principle calculations. The co-addition of Cu and Na increased the conversion efficiency of the devices. On the other hand, the device durability decreased, and this result was caused by the destabilization of the crystal structure due to the substitution of Cu and Na. The addition of stable EA greatly enhanced the durability of the device. These results indicate that the stabilizing effect of EA substitution on the crystal structure is also observed in the inclusion of Cu and Na.

## 2. Computational Conditions and Device Fabrication Methods

### 2.1. Computational Conditions

An example of the crystal structure model used in the first-principles calculations is shown in Figure 1. The composition of the perovskite crystal is represented as  $ABX_3$ , consisting of (A) organic cation, (B) metal cation, and (X) halogen anion. A total substitution structure model with a cell size of  $1 \times 1 \times 1$  and a partial substitution structure model with a cell size of  $2 \times 2 \times 2$ , as shown in Figure 1, were used in the calculations to study the effect of atomic or molecular substitution. The details of the calculation method are described in the previous papers [11,18–21].

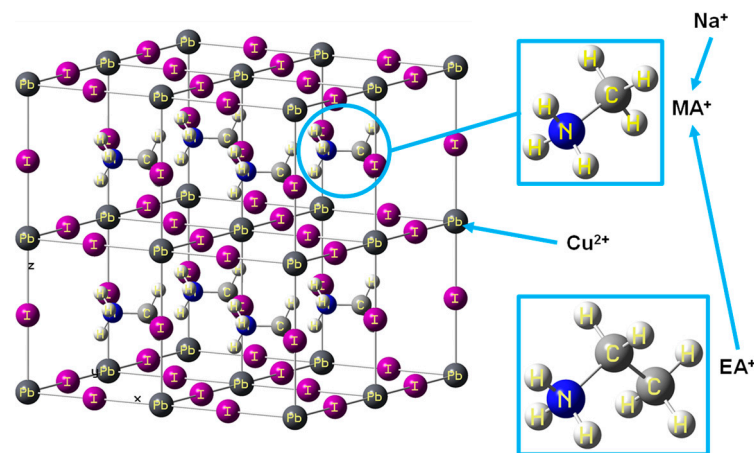


**Figure 1.**  $2 \times 2 \times 2$  crystal structure model and images of Cu, Na, and EA substitutions.

### 2.2. Device Fabrication Methods

The electron transport layer, perovskite layer, and hole transport layer were formed on the FTO substrate by spin coating and annealing, and finally, the device was fabricated by vacuum evaporation of gold. Details of the experimental methods are described in the previous papers [11,22–27].

## 3. Results and Discussion

### 3.1. Results of First-Principles Calculations

Figure 2 shows the calculated electron density distribution and confirms that the electron density around halogens increases in the order of iodine (I), bromine (Br), and chlorine (Cl). Table 1 also shows the calculated results for each structural model. It is suggested that substituting iodine with bromine or chlorine stabilizes the crystal structure and increases the energy gap. These results suggest that the addition of bromide or chloride is expected to enhance the device's durability and open-circuit voltage.

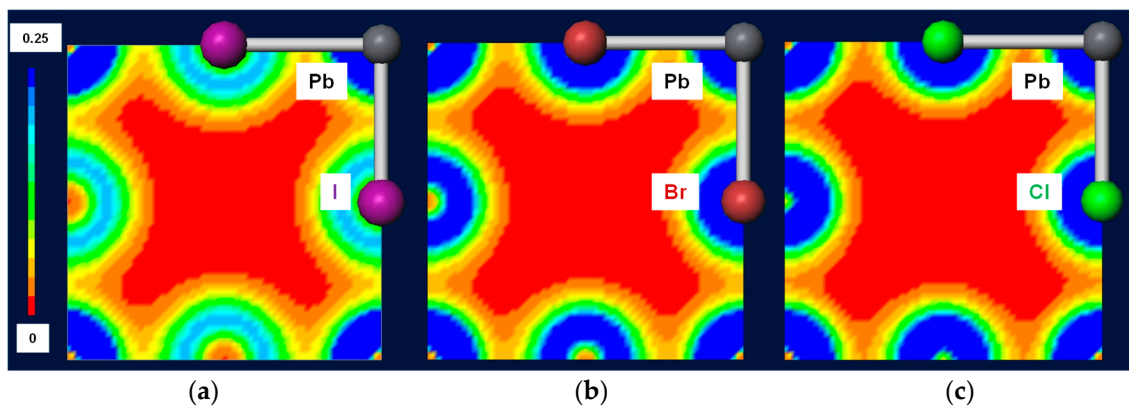


**Figure 2.** Calculated electron density distribution of (a) MAPbI<sub>3</sub>, (b) MAPbBr<sub>3</sub> and (c) MAPbCl<sub>3</sub>.

**Table 1.** Parameters of perovskite crystals obtained by first-principles calculations.

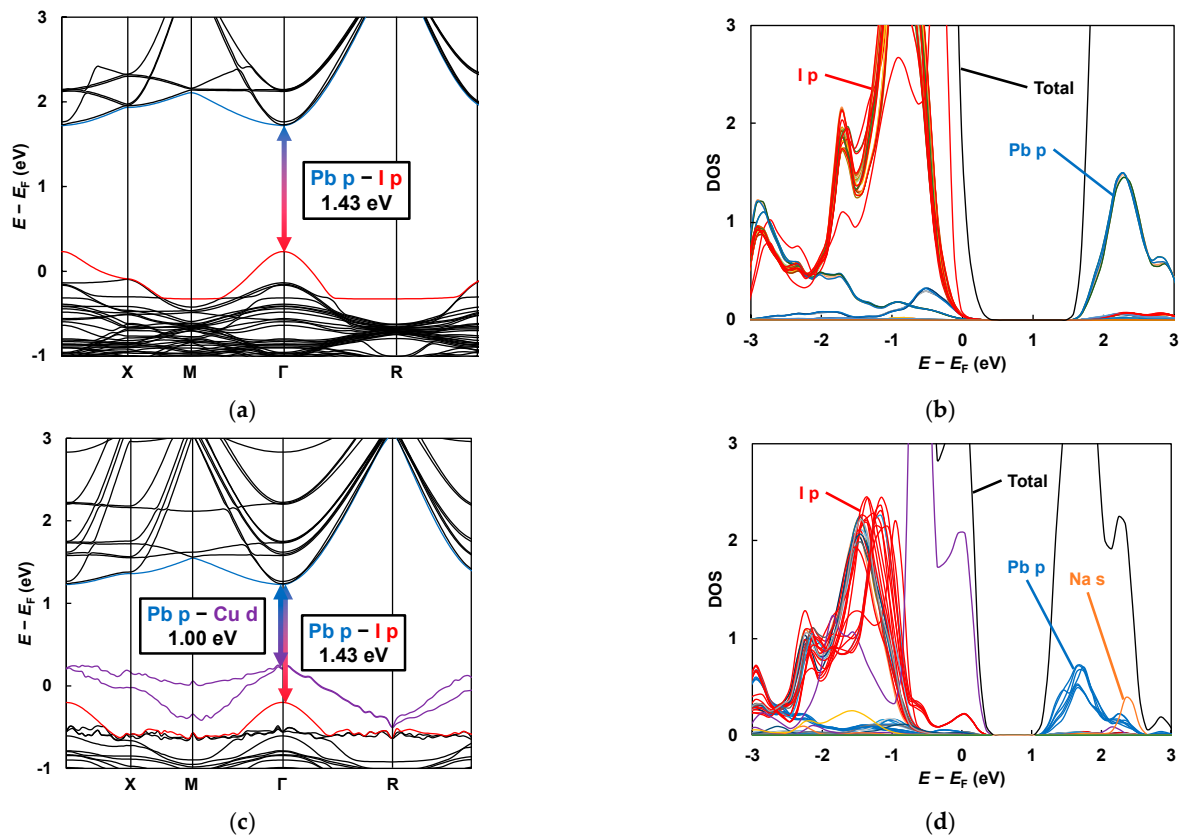
Model	Total Energy (keV)	Energy Gap (eV)	$m_e^*/m_0$	$m_h^*/m_0$
MAPbI <sub>3</sub>	−3.50	1.51	0.071	0.100
MAPbBr <sub>3</sub>	−3.66	2.26	0.224	0.100
MAPbCl <sub>3</sub>	−3.78	2.75	0.144	0.462

Figure 3 shows the calculated band structure and density of partial states, and Table 2 shows the calculated results. From DOS, the I-p orbital is dominant in the valence band and the Pb-p orbital is dominant in the conduction band, suggesting that charge is transferred between I-p and Pb-p. The Cu-d orbital derived from energy levels is formed in the forbidden band region, suggesting that charge carriers may be trapped and lost by recombination. The energy gap values reported in Table 1 suggest that the addition of the Cu compound is expected to lower the energy gap. The DOS confirms that the Na-s orbital-derived energy levels are far from the CBM. Since this level is isolated in the conduction band, it is not expected to be directly involved in charge transfer.

From the total energies, the substitution of lead (Pb) and MA with Cu and Na, respectively, is expected to destabilize the crystal structure. On the other hand, the substitution of MA with EA indicates that the crystal structure may be stabilized. Therefore, the introduction of EA into the Cu and Na systems is expected to be effective in terms of crystal structure stability.

**Table 2.** Parameters of perovskite crystals obtained by first-principles calculations.

Model	Total Energy (keV)	Energy Gap (eV)	$m_e^*/m_0$	$m_h^*/m_0$
MACuI <sub>3</sub>	−2.52	1.48	0.136	0.079
NaPbI <sub>3</sub>	−2.99	1.06	0.077	0.062
EAPbI <sub>3</sub>	−3.68	1.43	0.076	0.104
MA <sub>0.875</sub> EA <sub>0.125</sub> PbI <sub>3</sub>	−3.52	1.49	0.228	0.199
MA <sub>0.875</sub> EA <sub>0.125</sub> Pb <sub>0.875</sub> Cu <sub>0.125</sub> I <sub>3</sub>	−3.39	1.00	0.266	0.352
MA <sub>0.750</sub> EA <sub>0.125</sub> Na <sub>0.125</sub> Pb <sub>0.875</sub> Cu <sub>0.125</sub> I <sub>3</sub>	−3.32	1.04	0.241	0.355



**Figure 3.** Band structures and DOS of (a,b)  $\text{MA}_{0.875}\text{EA}_{0.125}\text{PbI}_3$ , (c)  $\text{MA}_{0.875}\text{EA}_{0.125}\text{Pb}_{0.875}\text{Cu}_{0.125}\text{I}_3$ , and (d)  $\text{MA}_{0.750}\text{EA}_{0.125}\text{Na}_{0.125}\text{Pb}_{0.875}\text{Cu}_{0.125}\text{I}_3$ .

### 3.2. Results of Experiments

Table 3 shows the results of the current-voltage characteristics of the fabricated devices. The simultaneous addition of Cu and Na significantly enhanced the conversion efficiency, which is mainly caused by the increase in the open-circuit voltage. From the calculation results shown in Table 1, it was predicted that the energy gap would increase with Br substitution. The results correspond to the experimental and calculated results. In general, the open-circuit voltage increases as the energy gap increases. Therefore, the increase in the energy gap due to Br substitution is considered to have contributed to the enhancement of the open-circuit voltage.

From Figure 3 and Table 2, it was predicted that the introduction of Cu would result in a loss of carriers and a decrease in the energy gap; however, the actual experimental addition of Cu enhanced the conversion efficiency and did not decrease the energy gap. Based on the above calculations and experimental results, we suggest that the Cu-d orbital level functions as an acceptor level; the creation of an excitation process from the I-p orbital level to the Cu-d orbital level enhances the generation of carriers, resulting in enhanced device properties.

**Table 3.** Parameters obtained by current-voltage characterization.

Devices	$J_{SC}$ ( $\text{mA cm}^{-2}$ )	$V_{OC}$ (V)	$FF$	$R_S$ ( $\Omega \text{ cm}^2$ )	$R_{Sh}$ ( $\Omega \text{ cm}^2$ )	$\eta$ (%)	$\eta_{ave}$ (%)	$E_g$ (eV)
Standard	22.2	0.739	0.497	4.18	383	8.17	5.82	1.55
CuBr <sub>2</sub> 2% NaBr 2%	21.7	0.841	0.578	5.93	594	10.5	8.36	1.56
CuBr <sub>2</sub> 2% NaBr 2% EABr 5%	21.3	0.843	0.585	5.12	558	10.5	8.67	1.57

Table 4 shows the results of the stability evaluation of the fabricated devices. The addition of Cu and Na decreased the stability of the devices compared to the standard devices, and the calculations shown in Table 2 indicate that the decrease in device durability is due to the destabilization of the crystal structure caused by the Cu and Na substitutions. The addition of EA to stabilize the crystal structure significantly enhanced the device's durability. Thus, it was confirmed that the stabilization effect of EA substitution is observed even in the inclusion of Cu and Na. The above calculations and experimental results suggest that the total energy values obtained by first-principles calculations may be used to estimate the device's durability.

**Table 4.** Changes of efficiencies of the present devices.

Devices	$\eta_{ave}$ (%)				Stability (%)
	0 Week	1 Week	2 Weeks	4 Weeks	
CuBr <sub>2</sub> 2% NaBr 2%	8.36	7.34	6.61	6.75	79.1
CuBr <sub>2</sub> 2% NaBr 2% EABr 5%	8.67	8.34	8.34	7.98	96.2

#### 4. Conclusions

In this study, the effects of Cu, Na, and EA additions were investigated by experiment and first-principles calculations. The addition of Cu and Na significantly enhanced the conversion efficiency of the devices. The result that the energy gap increases with bromine addition is in agreement with calculations and experiments, indicating that the bromine substitution contributed to the improvement of the open-circuit voltage. The calculated band structure and device properties also suggest that the Cu-d orbital level may function as an acceptor level. From the total energy, the crystal structure is predicted to be destabilized by the Cu and Na substitutions, and a decrease in device durability was also observed in experiments. The introduction of EA, a stable organic cation, to improve the stability of the crystal structure significantly enhanced the device's durability. The above calculations and experimental results suggest that the total energy obtained by first-principles calculations may be used to estimate the device's durability. The method described here for studying the effects of compound addition through calculation and experiment may be applicable to other alkali metals and organic cations.

**Author Contributions:** Conceptualization, R.O. and T.O.; Methodology, R.O., T.O. and A.S.; Formal Analysis, R.O., T.O. and A.S.; Investigation, R.O. and A.S.; Resources, M.O., S.F., T.T. and T.H.; Data Curation, R.O. and T.O.; Writing—Original Draft Preparation, R.O. and T.O.; Writing—Review and Editing, R.O., T.O., A.S., M.O., S.F., T.T. and T.H.; Project Administration, T.O.; Funding Acquisition, T.O. All authors have read and agreed to the published version of the manuscript.

**Funding:** This research was partly funded by Japan Society for the Promotion of Science as a Grant-in-Aid for Scientific Research (C) 21K04809.

**Institutional Review Board Statement:** Not applicable.

**Informed Consent Statement:** Not applicable.

**Data Availability Statement:** Data is contained within the article.

**Conflicts of Interest:** The authors declare no conflict of interest.

#### References

1. Wang, K.L.; Wang, R.; Wang, Z.K.; Li, M.; Zhang, Y.; Ma, H.; Liao, L.S.; Yang, Y. Tailored phase transformation of CsPbI<sub>2</sub>Br films by copper (II) bromide for high-performance all-inorganic perovskite solar cells. *Nano Lett.* **2019**, *19*, 5176–5184. [[CrossRef](#)]
2. Jahandar, M.; Heo, J.H.; Song, C.E.; Kong, K.J.; Shin, W.S.; Lee, J.C.; Im, S.H.; Moon, S.J. Highly efficient metal halide substituted CH<sub>3</sub>NH<sub>3</sub>I(PbI<sub>2</sub>)<sub>1-x</sub>(CuBr<sub>2</sub>)<sub>x</sub> planar perovskite solar cells. *Nano Energy* **2016**, *27*, 330–339. [[CrossRef](#)]
3. Li, M.; Wang, Z.K.; Zhuo, M.P.; Hu, Y.; Hu, K.H.; Ye, Q.Q.; Jain, S.M.; Yang, Y.G.; Gao, X.Y.; Liao, L.S. Pb–Sn–Cu Ternary organometallic halide perovskite solar cells. *Adv. Mater.* **2018**, *30*, 1800258. [[CrossRef](#)] [[PubMed](#)]

4. Qiao, L.; Fang, W.H.; Long, R.; Prezhdo, O.V. Alkali metals extend carrier lifetimes in lead halide perovskites by passivating and eliminating halide interstitial defects. *Angew. Chem.* **2020**, *132*, 4714–4720. [[CrossRef](#)]
5. Oku, T.; Kandori, S.; Taguchi, M.; Suzuki, A.; Okita, M.; Minami, S.; Fukunishi, S.; Tachikawa, T. Polysilane-inserted methylammonium lead iodide perovskite solar cells doped with formamidinium and potassium. *Energies* **2020**, *13*, 4776. [[CrossRef](#)]
6. Kandori, S.; Oku, T.; Nishi, K.; Kishimoto, T.; Ueoka, N.; Suzuki, A. Fabrication and characterization of potassium- and formamidinium-added perovskite solar cells. *J. Ceram. Soc. Jpn.* **2020**, *128*, 805. [[CrossRef](#)]
7. Kim, S.G.; Li, C.; Guerrero, A.; Yang, J.M.; Zhong, Y.; Bisquert, J.; Huettner, S.; Park, N.G. Potassium ions as a kinetic controller in ionic double layers for hysteresis-free perovskite solar cells. *J. Mater. Chem. A* **2019**, *7*, 18807. [[CrossRef](#)]
8. Correa-Baena, J.P.; Luo, Y.; Brenner, T.M.; Snider, J.; Sun, S.; Li, X.; Jensen, M.A.; Hartomo, N.T.P.; Nienhaus, L.; Wieghold, S.; et al. Homogenized halides and alkali cation segregation in alloyed organic-inorganic perovskites. *Science* **2019**, *363*, 627–631. [[CrossRef](#)]
9. Ueoka, N.; Oku, T. Effects of co-addition of sodium chloride and copper (II) bromide to mixed-cation mixed-halide perovskite photovoltaic devices. *ACS Appl. Energy Mater.* **2020**, *3*, 7272–7283. [[CrossRef](#)]
10. Ueoka, N.; Oku, T.; Suzuki, A. Additive effects of alkali metals on Cu-modified  $\text{CH}_3\text{NH}_3\text{PbI}_{3-\delta}\text{Cl}_\delta$  photovoltaic devices. *RSC Adv.* **2019**, *9*, 24231–24240. [[CrossRef](#)] [[PubMed](#)]
11. Okumura, R.; Oku, T.; Suzuki, A.; Okita, M.; Fukunishi, S.; Tachikawa, T.; Hasegawa, T. Effects of Adding Alkali Metals and Organic Cations to Cu-Based Perovskite Solar Cells. *Appl. Sci.* **2022**, *12*, 1710. [[CrossRef](#)]
12. Liu, D.; Li, Q.; Wu, K. Ethylammonium as an alternative cation for efficient perovskite solar cells from first-principles calculations. *RSC Adv.* **2019**, *9*, 7356. [[CrossRef](#)] [[PubMed](#)]
13. Mateen, M.; Arain, Z.; Liu, X.; Iqbal, A.; Ren, Y.; Zhang, X.; Liu, C.; Chen, Q.; Ma, S.; Ding, Y.; et al. Boosting optoelectronic performance of  $\text{MAPbI}_3$  perovskite solar cells via ethylammonium chloride additive engineering. *Sci. China Mater.* **2020**, *63*, 2477–2486. [[CrossRef](#)]
14. Nishi, K.; Oku, T.; Kishimoto, T.; Ueoka, N.; Suzuki, A. Photovoltaic characteristics of  $\text{CH}_3\text{NH}_3\text{PbI}_3$  perovskite solar cells added with ethylammonium bromide and formamidinium iodide. *Coatings* **2020**, *10*, 410. [[CrossRef](#)]
15. Mohebpour, M.A.; Saffari, M.; Soleimani, H.R.; Tagani, M.B. High performance of mixed halide perovskite solar cells: Role of halogen atom and plasmonic nanoparticles on the ideal current density of cell. *Phys. E* **2018**, *97*, 282–289. [[CrossRef](#)]
16. Lee, A.Y.; Park, D.Y.; Jeong, M.S. Correlational study of halogen tuning effect in hybrid perovskite single crystals with Raman scattering, X-ray diffraction, and absorption spectroscopy. *J. Alloys Compd.* **2018**, *738*, 239–245. [[CrossRef](#)]
17. Motta, C.; El-Mellouhi, F.; Sanvito, S. Charge carrier mobility in hybrid halide perovskites. *Sci. Rep.* **2015**, *5*, 12746. [[CrossRef](#)]
18. Suzuki, A.; Kishimoto, K.; Oku, T.; Okita, M.; Fukunishi, S.; Tachikawa, T. Additive effect of lanthanide compounds into perovskite layer on photovoltaic properties and electronic structures. *Synth. Met.* **2022**, *287*, 117092. [[CrossRef](#)]
19. Kishimoto, T.; Oku, T.; Suzuki, A.; Ueoka, N. Additive effects of guanidinium iodide on  $\text{CH}_3\text{NH}_3\text{PbI}_3$  perovskite solar cells. *Phys. Status Solidi A* **2021**, *218*, 2100396. [[CrossRef](#)]
20. Suzuki, A.; Oku, T. Effects of mixed-valence states of Eu-doped  $\text{FAPbI}_3$  perovskite crystals studied by first-principles calculation. *Mater. Adv.* **2021**, *2*, 2609–2616. [[CrossRef](#)]
21. Ono, I.; Oku, T.; Suzuki, A.; Asakawa, Y.; Terada, S.; Okita, M.; Fukunishi, S.; Tachikawa, T. Fabrication and characterization of  $\text{CH}_3\text{NH}_3\text{PbI}_3$  solar cells with added guanidinium and inserted with decaphenylpentasilane. *Jpn. J. Appl. Phys.* **2022**, *61*, SB1024. [[CrossRef](#)]
22. Oku, T.; Ohishi, Y.; Ueoka, N. Highly (100)-oriented  $\text{CH}_3\text{NH}_3\text{PbI}_3(\text{Cl})$  perovskite solar cells prepared with  $\text{NH}_4\text{Cl}$  using an air blow method. *RSC Adv.* **2018**, *8*, 10389–10395. [[CrossRef](#)]
23. Taguchi, M.; Suzuki, A.; Oku, T.; Ueoka, N.; Minami, S.; Okita, M. Effects of annealing temperature on decaphenylcyclopentasilane-inserted  $\text{CH}_3\text{NH}_3\text{PbI}_3$  perovskite solar cells. *Chem. Phys. Lett.* **2019**, *737*, 136822. [[CrossRef](#)]
24. Suzuki, A.; Taguchi, M.; Oku, T.; Okita, M.; Minami, S.; Fukunishi, S.; Tachikawa, T. Additive effects of methyl ammonium bromide or formamidinium bromide in methylammonium lead iodide perovskite solar cells using decaphenylcyclopentasilane. *J. Mater. Sci. Mater. Electron.* **2021**, *32*, 26449–26464. [[CrossRef](#)]
25. Oku, T.; Taguchi, M.; Kandori, S.; Suzuki, A.; Okita, M.; Minami, S.; Fukunishi, S.; Tachikawa, T. Effects of polysilane addition to chlorobenzene and high temperature annealing on  $\text{CH}_3\text{NH}_3\text{PbI}_3$  perovskite photovoltaic devices. *Coatings* **2021**, *11*, 665. [[CrossRef](#)]
26. Enomoto, A.; Suzuki, A.; Oku, T.; Okita, M.; Fukunishi, S.; Tachikawa, T.; Hasegawa, T. Effects of Cu, K and guanidinium addition to  $\text{CH}_3\text{NH}_3\text{PbI}_3$  perovskite solar cells. *J. Electron. Mater.* **2022**, *51*, 4317–4328. [[CrossRef](#)]
27. Huang, L.; Hu, Z.; Xu, J.; Zhang, K.; Zhang, J.; Zhu, Y. Multi-step slow annealing perovskite films for high performance planar perovskite solar cells. *Sol. Energy Mater. Sol. Cells* **2015**, *141*, 377–382. [[CrossRef](#)]